Innovative Food Science and Emerging Technologies 47 (2018) 56–70

Contents lists available at ScienceDirect

Innovative Food Science and Emerging Technologies

journal homepage: www.elsevier.com/locate/ifset

Radio frequency heating uniformity evaluation for mid-high moisture food treated with cylindrical electromagnetic wave conductors

Hankun Zhu[a], Dong Li[a], Jiwei Ma[b], Zhilong Du[b], Peigang Li[b], Shujun Li[a,c,*], Shaojin Wang[d,e,**]

[a] College of Engineering, China Agricultural University, Beijing 100083, China
[b] Chinese Academy of Agricultural Mechanization Sciences, Beijing 100083, China
[c] Department of Central Research and Development, China National Machinery Industry Corporation, Beijing 100080, China
[d] College of Mechanical and Electronic Engineering, Northwest A&F University, Yangling, Shaanxi 712100, China
[e] Washington State University, Department of Biological Systems Engineering, Pullman, WA 99164-6120, USA

ARTICLE INFO

Keywords:
Mid-high moisture food
Uniformity
Electromagnetic
RF
EWC
Simulation

ABSTRACT

Non-uniform heating is an important obstacle for applying radio frequency (RF) energy in food processing, especially for the material with high moisture content. To further extend wide applications of the RF heating uniformity improvement based on our previous study with cross electromagnetic wave conductor (EWC), a novel and effective method with cylindrical electromagnetic wave conductors and cylindrical containers was introduced in this study to improve the electromagnetic energy distribution inside the sample with mid-high moisture content. The associated computer simulation model with cylindrical EWC and container was also developed and validated based on RF experimental results to evaluate the heating uniformity. The results showed that the parameters of EWC (diameter and height) had a positive effect on the RF heating uniformity index. The sample treated with cylindrical EWC had better heating uniformity but lower temperature than that treated with cross EWC based on the comparison results. The improved target uniformity index (TUI) and the decreased heating time also indicated the positive effects of cylindrical EWC. A simplified structure for cylindrical EWC was developed and evaluated by computer simulation, which may provide potential applications of the cylindrical EWC to achieve the required RF heating uniformity in mid-high moisture food.

1. Introduction

Recently, electromagnetic dielectric treatment methods (microwave and radio frequency) have gained special attentions in food processing as the alternative thermal treatment method due to the high heating efficiency, short treatment time and low operational cost (Chandrasekaran, Ramanathan, & Basak, 2013; Marra, Zhang, & Lyng, 2009). In comparison with the microwave treatment, radio frequency (RF) energy has better volumetric heating and deeper penetration, especially for processing large bulk food materials (Jiao, Tang, & Wang, 2014; Wang et al., 2011; Wang & Tang, 2001). Many studies on RF treatments have been applied for food processing, including disinfestations (Wang, Tiwari, Jiao, Johnson, & Tang, 2010), pasteurization (Liu et al., 2011; Zheng, Zhang, & Wang, 2017), drying (Wang et al., 2011; Zhang, Zheng, Zhou, Huang, & Wang, 2016), thawing (Bedane, Chen, Marra, & Wang, 2017; Erdogdu, Altin, Marra, & Bedane, 2017) and baking (Koral, 2004). However, the main barrier for RF treatments is the non-uniform heating, especially for the materials with high moisture content (Huang, Zhang, Marra, & Wang, 2016; Zhu, Li, Li, & Wang, 2017), which causes large cold spot areas and overheating parts in the treated samples (Huang, Zhu, Yan, & Wang, 2015) and results in either survivals of pathogens/insects or degraded product quality (Huang et al., 2016).

Many studies have been carried out to improve the RF heating uniformity and can be mainly summarized into three approaches: 1) using additional assistance strategies to maintain a suitable ambient temperature or move the material during RF treatment (Birla, Wang, Tang, & Hallman, 2004; Chen, Wang, Li, & Wang, 2015; Hou, Ling, & Wang, 2014); 2) adjusting the top electrode shape, movement, geometry and position of the sample (Alfaifi et al., 2014; Alfaifi, Tang, Rasco, Wang, & Sablani, 2016; Tiwari, Wang, Tang, & Birla, 2011a; Uyar, Erdogdu, Sarghini, & Marra, 2016); 3) using additional surrounding materials, such as polyetherimide (Jiao, Shi, Tang, Li, & Wang, 2015), polystyrene (Huang et al., 2016) and mica (Zhang, Huang, & Wang, 2017) around the sample to modify the electromagnetic field distribution. These methods are effective to improve the

* Correspondence to: S. Li, College of Engineering, China Agricultural University, Beijing 100083, China.
** Correspondence to: S. Wang, College of Mechanical and Electronic Engineering, Northwest A&F University, Yangling, Shaanxi 712100, China.
E-mail addresses: lisj@caams.org.cn (S. Li), shaojinwang@nwsuaf.edu.cn (S. Wang).

https://doi.org/10.1016/j.ifset.2018.01.010
Received 5 July 2017; Received in revised form 21 January 2018; Accepted 24 January 2018

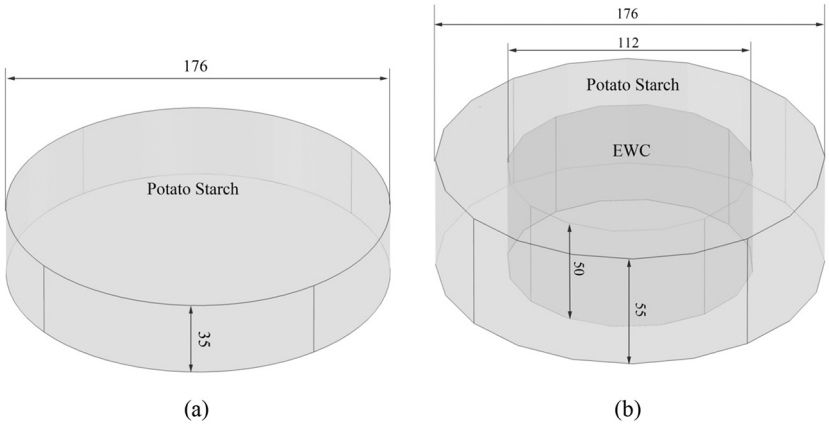

Fig. 1. Sketches of the sample in the cylindrical container without (a) and with cylindrical EWC (b) (all dimensions are in mm).

Table 1
Electrical and physical properties of polystyrene, polypropylene, air, and aluminum used in simulation modeling.

Container and surrounding material	Density ($kg\,m^{-3}$)	Thermal conductivity ($W\,m^{-1}\,K^{-1}$)	Heat capacity ($J\,kg^{-1}\,K^{-1}$)	Dielectric constant (ε')	Loss factor (ε'')
Polystyrene	25[a]	0.036[a]	1300[a]	2.6[b]	0.0003[b]
Polypropylene[c]	900	0.26	1800	2.0	0.0023
Air[d]	1.2	0.025	1200	1	0
Aluminum[d]	2700	160	900	1	0

[a] Juran (1991).
[b] Brandrup, Immergut, Grulke, Abe, and Bloch (1989)..
[c] Von Hippel (1954).
[d] COMSOL materail labrary (COMSOL, 2012).

RF heating uniformity are mostly limited to low-moisture food materials (< 20% w.b.). This is probably caused by the relatively narrow temperature variation over the low moisture sample with the low dielectric loss factor values. For the food material with high moisture level (> 60% w.b.), such as fresh fruit, Birla et al. (2004) introduced a fruit mover with fruit immersion and rotation using circulated water during RF heating to improve the RF heating uniformity. But for the food material with mid-high moisture levels (20%–60% w.b.), it is difficult to manipulate the current results for practical applications. It's desirable to explore a simple, convenient and suitable method for improving RF heating uniformity in mid-high moisture food.

For this reason, a new RF heating uniformity improving method for mid-high moisture food materials based on the RF electromagnetic field distribution and bending theory (Birla et al., 2004; TEC, 1987) was developed in our previous study (Zhu et al., 2017), in which a polystyrene made crossed electromagnetic wave conductor (EWC) sheet was introduced at the central area of the rectangular container inside the sample. The EWC effectively improved RF electromagnetic distribution uniformity and heating efficiency. However, large temperature deviations still existed in the superficial area of the sample with rectangular container and cross EWC, because of the intensification of the heating occurred at the edge and corner parts, due to the energy converging effect at angle parts, especially for the material with high moisture content (TEC, 1987). To continually extend and promote wide applications of the EWC method, a new EWC type with less edges and corners are needed to achieve the uniform RF heating patterns.

The objectives of this study were 1) to develop a new cylindrical EWC with cylindrical container for RF treatments, 2) to compare the RF heating patterns between the sample heated with cross and equivalent cylindrical EWC, 3) to evaluate the RF heating effect on the sample with cylindrical EWC, and 4) to explore a simple cylindrical EWC structure for practical applications in RF treated mid-high moisture food.

2. Materials and methods

2.1. Sample preparation

Standard refined potato starch (Maoyuan Inc., Pingliang, Gansu, China) was used as representative mid-high moisture food in this study with initial moisture content of 11.28% w.b. To get the same moisture content with previous study (Zhu et al., 2017) for comparison, the moisture content was adjusted to 31.55% w.b. by adding predetermined quantity of distilled water. The preconditioned samples were gently mixed and shaken manually for 15 min. The sample was sealed in an isolated air-tight plastic bag at 4 °C for 4 days in a refrigerator to balance the moisture, and the bags were shaken 3 times per day during storage. The sample bags were taken out from the refrigerator after equilibrium and put in an incubator (BSC-150, Shanghai BoXun Industrial & Commerce Co., LTD., Shanghai, China) at 23 °C for one more day to obtain uniform initial sample temperature before the experiment (Huang et al., 2016; Wang, Zhu, Chen, Li, & Wang, 2015).

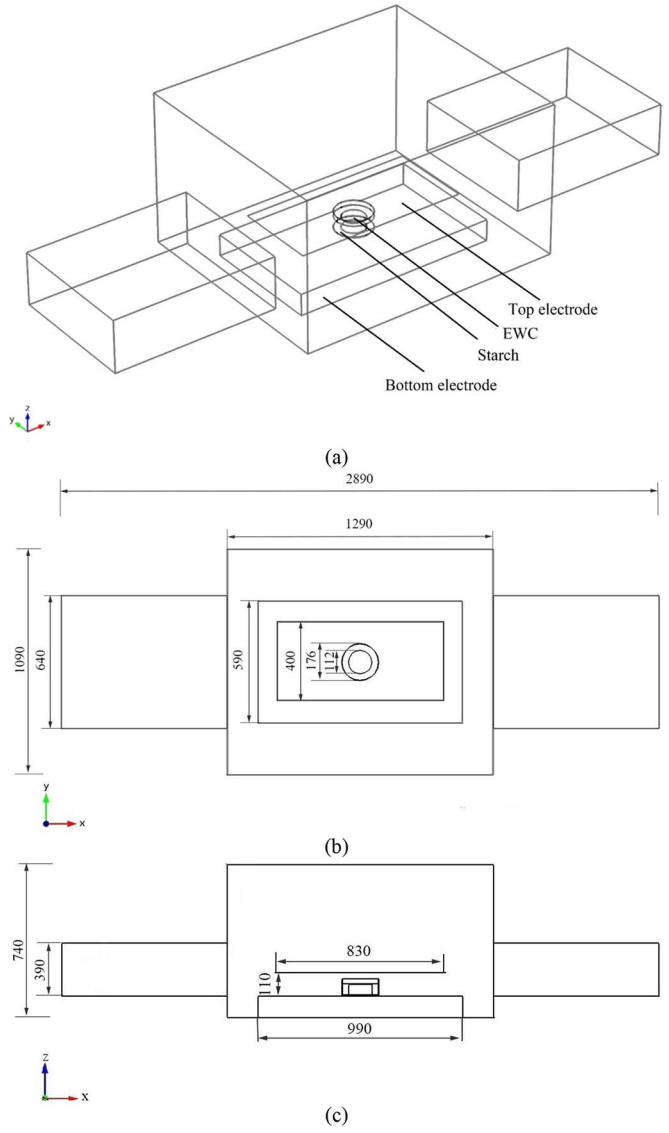

Fig. 2. 3-D geometry (a) and dimensions (b, c) of the cylindrical sample with EWC in the RF cavity (all dimensions are in mm).

2.2. Design of EWC

In the previous study, a polystyrene made cross EWC was introduced into potato starch samples for its low loss factor, thermal conductivity and low water absorption to improve the RF heating uniformity, and the electromagnetic distribution was obviously changed inside the rectangular sample (Zhu et al., 2017). In this study, a new polystyrene made cylindrical EWC at the concentric position of a cylindrical polypropylene container was introduced and explored, and the comparison test of the RF heating effect between the cylindrical EWC and the cross EWC was also conducted based on same treatment parameters (container bottom area, EWC bottom area, EWC height and heating time) to make sure that with the same sample quantity or volume was obtained by changing the sample height and the cyclical EWC size. The schematic diagram of the sample with cylindrical EWC was shown in Fig. 1.

2.3. Physical properties used in the computer simulation

Physical parameters of the potato starch including dielectric properties, bulk density, thermal conductivity and heat capacity used in the simulation model were referred to Zhu et al. (2017). Physical properties of the container, and surrounding materials, including polystyrene (EWC), polypropylene (container), aluminum (RF system), and air used in computer simulation model were listed in Table 1.

2.4. Computer simulation

2.4.1. Physical model of RF heating

The RF system was mainly constituted by a RF generator and heating cavity. RF energy was generated by a high voltage rectifying and inverter circuits in the generator and then matched into heating circuit with two parallel electrodes through a feeding strip at the heating cavity. High intensity electromagnetic field was formed between two parallel electrodes, and the adjustable electrode gap determines different output power in the dielectric materials (samples). The sample (potato starch and EWC) was placed on the center part of bottom electrode (Fig. 2). The size of polypropylene cylindrical container was 176 mm diameter and 80 mm height. The electrode gap used in the model was set at 110 mm.

2.4.2. Governing equations

RF simulation was based on the simultaneous solution of heat transfer coupled with electromagnetic field displacement in the multi-domains, including the surrounding, container, sample and EWC part inside the RF cavity. Electromagnetic field distribution inside the RF applicator was described by four Maxwell's equations of electromagnetism in differential forms, which could be expressed in terms of the electric field (E) and magnetic intensity (H) as follows (Balanis, 1989):

$$\nabla \cdot \vec{D} = \rho_e \tag{1}$$

$$\nabla \cdot \vec{B} = 0 \tag{2}$$

$$\nabla \cdot \vec{E} = \frac{\partial \vec{B}}{\partial t} = \mu \frac{\partial \vec{H}}{\partial t} \tag{3}$$

$$\nabla \cdot \vec{H} = \vec{J} + \frac{\partial \vec{D}}{\partial t} = \varepsilon_0 \varepsilon'' \omega \vec{E} \tag{4}$$

where D is the electric flux density ($C\,m^{-2}$), B is the magnetic flux density ($Wb\,m^{-2}$), ρ_e is the total electric charge density ($C\,m^{-3}$), E is the electric field intensity ($V\,m^{-1}$), H is the magnetic field intensity ($A\,m^{-1}$), μ is the magnetic permeability ($H\,m^{-1}$), J is the total current density ($A\,m^{-2}$), ω is the angular frequency ($rad\,s^{-1}$), and ε is the complex relative permittivity of the dielectric material ($F\,m^{-1}$), which can be expressed in terms of the relative (to air) dielectric constant (ε') and the relative loss factor (ε'') of the material ($\varepsilon = \varepsilon' - j\varepsilon'$). The absorbed RF power density and conversion at any point inside the material is proportional to the square of the electric field strength, the dielectric loss factor and the frequency as follows (Choi & Konrad, 1991; Jiao et al., 2015):

$$Q = 2\pi f \varepsilon_0 \varepsilon'' E_r^2 = \pi f \varepsilon_0 \varepsilon'' |\vec{E}|^2 \tag{5}$$

where Q is the power conversion to thermal energy in foods ($W\,m^{-3}$), f is the frequency (Hz), ε_0 is the permittivity of electromagnetic wave in free space ($8.86 \times 10^{-12}\,F\,m^{-1}$), E_r is the root mean square value of

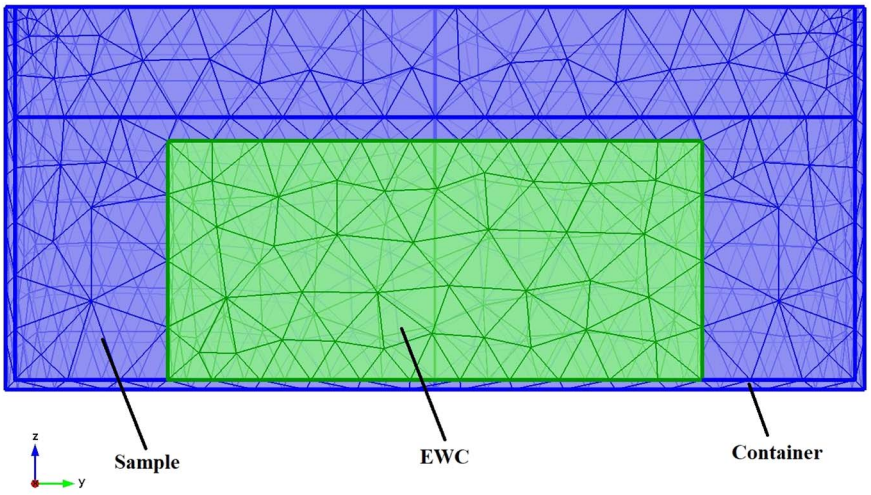

(a)

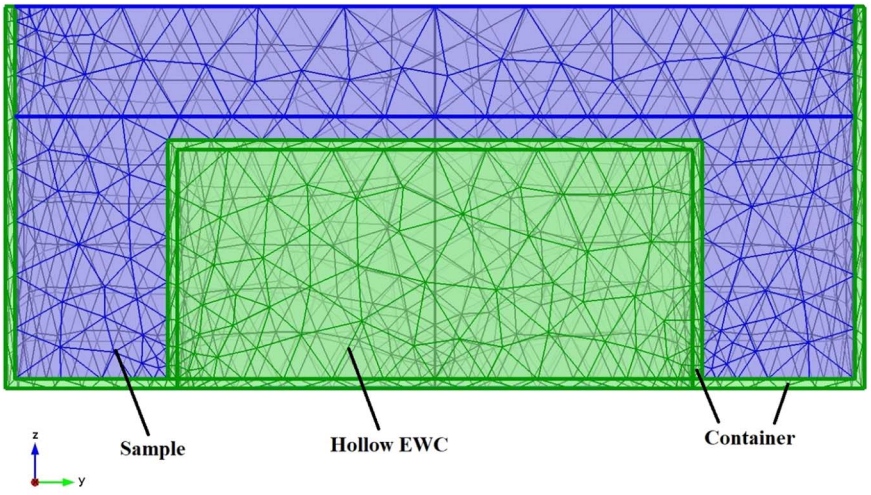

(b)

Fig. 3. Approach of potato starch with solid (a) and hollow (b) EWC in the simulation.

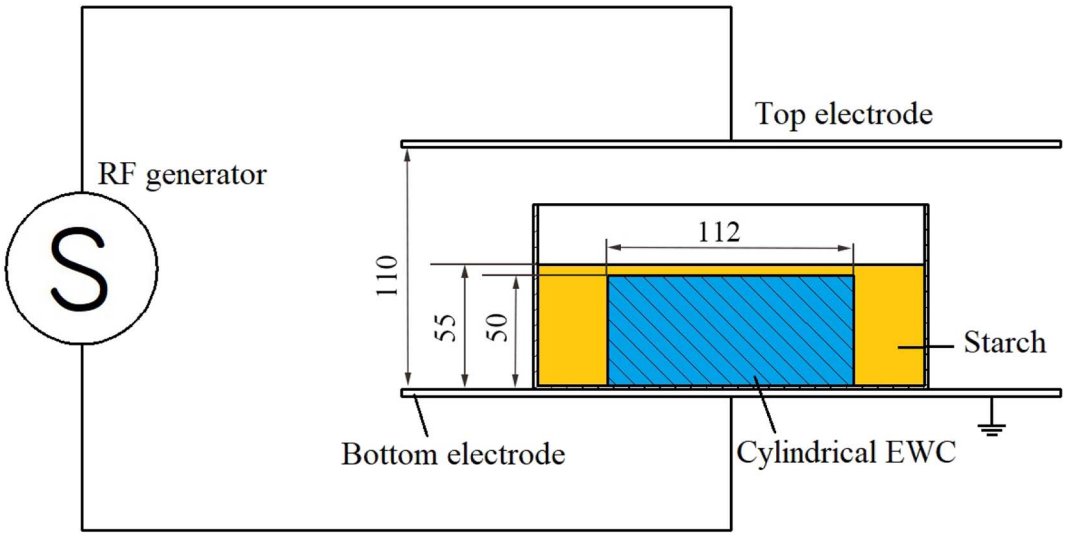

Fig. 4. Schematic of RF heating for potato starch at moisture content of 31.55% with cylindrical EWC (all dimensions are in mm).

Table 2
Associated RF treatment time (s) without and with different sizes of cylindrical EWC for the potato starch with moisture content of 31.55% w.b.

EWC diameter (mm)	EWC height (mm)					Without EWC
	20	30	40	50	60	
112	267	230	185	178	167	340
96	280	240	209	195	–	
76	325	290	260	–	–	

the electric field ($V\,m^{-1}$), and the scalar voltage potential (V) is related to the electric field as $\vec{E} = -\vec{\nabla}V$ Heat convection at the material's surface and the heat conduction within the sample (starch), is described by the equation (Nelson, 1996):

$$\rho C_p \frac{\partial T}{\partial t} = \vec{\nabla}\cdot k\vec{\nabla}T + Q \tag{6}$$

where $^{\partial T}/_{\partial t}$ is the heating rate in food material ($°C\,s^{-1}$), α is the thermal diffusivity ($m^2\,s^{-1}$), and ρ and C_p are the density ($kg\,m^{-3}$) and heat capacity ($J\,kg^{-1}\,K^{-1}$), respectively.

Convective heat transfer was considered on the external surface of the sample, which can be described as (Huang et al., 2015):

$$-k\vec{\nabla}T\vec{n} = h(T - T_{air}) \tag{7}$$

where h is convective heat transfer coefficient ($h = 20\,W\,m^{-2}K^{-1}$ for natural convection), T_{air} is the air temperature (≈23 °C) and $\vec{n}$ is the vector of the surface crossed by the heat flux.

2.4.3. Initial and boundary conditions

The metal enclosure boundary of RF unit was considered as thermal insulation ($\nabla T = 0$). The top electrode was set as the electromagnetic source since the electromagnetic energy was introduced by feeding strip from RF generator to the top electrode, and the voltage of the top electrode can be determined by anode current (I_a) with the equation as follows (Zhu, Huang, & Wang, 2014; Wang, Chen, Li, & Wang, 2015).

$$V = 10401 \times I_a + 1974.1 \tag{8}$$

The bottom electrode was set as ground ($V = 0$ V). Electrical insulation $\vec{\nabla}\cdot\vec{E} = 0$ was considered for the external walls of the RF cavity. The surrounding air was considered in the inlet and outlet of the system with condition of $T = T_{air}$. The initial temperature of all domains in the system, including the air, plastic container, starch, upper and bottom electrodes was set at 23 °C.

2.4.4. Solving and meshing procedure

A DELL workstation with Core i7 processors, 12 GB RAM on a Windows 7 64 bit operating system was used to run the finite element software COMSOL (V4.3a, COMSOL Multiphysics, Burlington, MA, USA). For solving the equations, frequency transient solver was chosen to evaluate the RF multi-physics heating model and evaluate the heating pattern of the sample during the heating period with the relative tolerance of 0.01. Finer tetrahedral mesh was generated in the sample, EWC (solid and hollow) and the top electrode to guarantee the accuracy of temperature distribution results (Fig. 3). For the model with solid EWC of 50 mm height and 112 mm diameter, the maximum and minimum element sizes were 159 and 11.6 mm, respectively, and the number of the all elements in the model was 38,142. For the model with hollow EWC of 50 mm height and 112 mm diameter (refer to Section 2.8), same mesh size was used in according with the solid EWC model, and the elements number was 43,882. Other parts (shell, bottom electrode and vestibule) of the model were meshed with normal size tetrahedral meshes. Mesh size was chosen based on the convergence study when the difference in the resulted temperatures between successive calculations was < 0.1% (Tiwari, Wang, Tang, & Birla, 2011b). The initial and maximum time steps used in this study were set as 0.001 and 1 s, respectively.

2.5. RF heating experiment

A 6 kW free-running oscillator RF system (SO6B, Strayfield International, Wokingham, UK) was used for RF heating experiment, and the schematic diagram was shown in Fig. 4. The cylindrical EWC with different sizes were placed inside the sample at the central area of a cylindrical polypropylene container. To make the comparison with previous experiments of cross EWC, same height of each sample was maintained based on the same container and EWC bottom areas. Therefore, the diameter of the cylindrical container used in this study was 176 mm and the cylindrical EWC diameters were 112 mm, 96 mm and 75 mm, respectively, corresponding to the previously used cross EWC widths of 35 mm, 25 mm and 15 mm. Each of the samples was divided into 2 layers based on the half of the weight by a gauze (with mesh opening of 0.7 mm) for easily mapping the surface sample temperature in each layer. The samples with cylindrical EWC were also

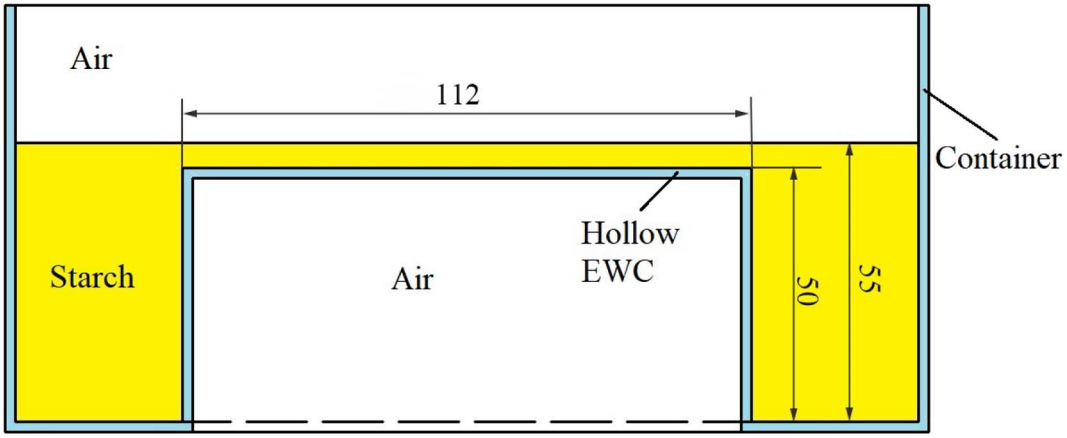

Fig. 5. Schematic of RF heating for potato starch with specific designed polypropylene container with cylindrical hollow EWC (all dimensions are in mm).

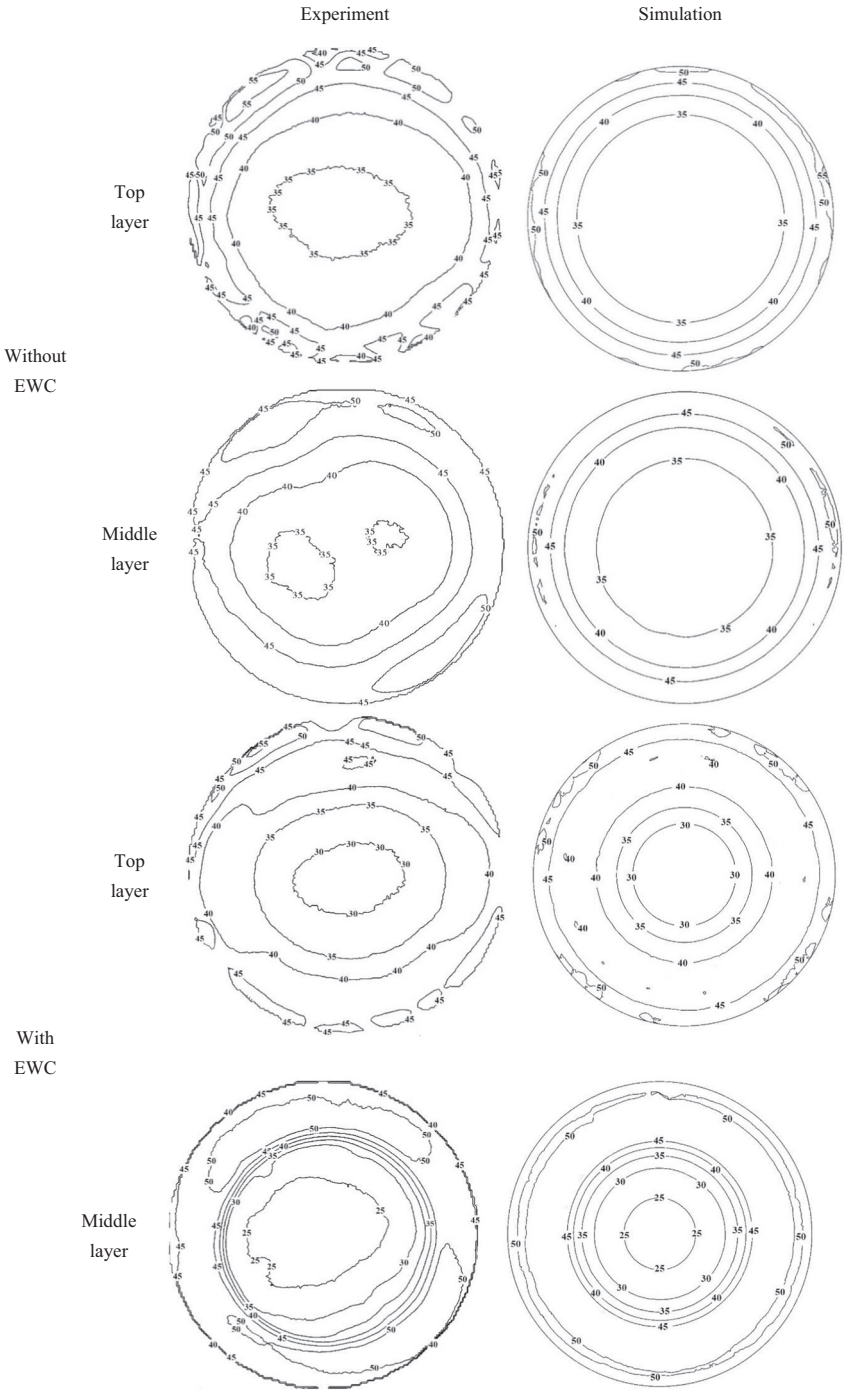

Fig. 6. Simulated and experimental temperature distributions (°C) of potato starch with moisture contents of 31.55% w.b. in top and middle layers placed in the polypropylene cylindrical container on the center of bottom electrode after RF heating at the electrode gap of 110 mm and initial temperature of 23 °C without and with cylindrical EWC (112 mm diameter and 50 mm height).

placed on the center of the bottom electrode with 110 mm electrode gap, and the RF heating time of the experiments was the same with the previous study. The container was immediately moved out after RF heating for temperature mapping with an infrared thermal imaging camera (DM63, Dali Science and Technology, Hangzhou, Zhejiang, China) with an accuracy of ± 2 °C. Each experiment was repeated two times.

2.6. EWC effect on RF heating uniformity

2.6.1. Heating uniformity evaluation

Heating uniformity of RF treatments with different types of EWC can be evaluated by the following two common indexes from the literature. The heating Uniformity Index (UI) developed by Alfaifi et al. (2014) was particularly used for the EWC heating effect comparison

Table 3
Simulated minimum (Min), maximum (Max), average (Avg) and standard deviation (Std) temperatures (°C) of potato starch with moisture content of 31.55% w.b. in two horizontal layers (top and middle) with various EWC diameters and determined height of 30 mm after RF heating with a fixed electrode gap of 110 mm and initial temperature of 23 °C.

EWC diameter (mm)	Layer	Min (°C)	Max (°C)	Avg (°C)	Std (°C)
Without	Top	30.34	52.94	41.36	6.82
	Mid	32.65	50.45	41.78	6.26
76	Top	27.92	52.74	40.76	6.95
	Mid	42.21	50.01	45.99	2.86
96	Top	27.21	54.24	41.81	7.25
	Mid	45.16	50.05	47.70	1.78
112	Top	26.30	51.38	40.99	7.73
	Mid	45.37	50.35	48.28	1.28

Table 4
Simulated minimum (Min), maximum (Max), average (Avg) and standard deviation (Std) temperatures (°C) of potato starch with moisture content of 31.55% w.b. in two horizontal layers (top and middle) with various EWC heights at determined diameter of 112 mm after RF heating with a fixed electrode gap of 110 mm and initial temperature of 23 °C.

EWC height (mm)	Layer	Min (°C)	Max (°C)	Avg (°C)	Std (°C)
20	Top	26.86	50.34	39.76	7.90
	Mid	26.83	50.10	42.87	7.78
30	Top	26.30	51.38	40.99	7.73
	Mid	45.37	50.35	48.28	1.28
40	Top	25.76	53.89	39.57	8.26
	Mid	47.41	50.26	49.06	0.74
50	Top	25.38	51.59	41.59	7.33
	Mid	46.93	50.45	49.24	0.73
60	Top	37.76	50.92	41.51	3.72
	Mid	45.91	50.28	48.84	0.95

with the equivalent size between cylindrical and cross EWC.

$$UI = \frac{\int_{Vvol} |T - T_{ave}|\ dV_{vol}}{(T_{ave} - T_{initial})V_{vol}} \quad (9)$$

where T is the local temperature in the sample (°C), $T_{initial}$ is the initial temperature of the sample (°C), T_{ave} is the average temperature of the volume (°C), and V_{vol} is the volume of food (m^3).

The target uniformity index (TUI) developed by Jiao et al. (2015) was particularly used for deviation of RF heating temperatures with different cylindrical EWC and target temperature:

$$TUI = \frac{\int_{Vvol} |T - T_t|\ dV_{vol}}{(T_t - T_{initial})V_{vol}} \quad (10)$$

where T_t is the target heating temperature (°C). Smaller uniformity index indicated better heating uniformity for the selected domain in simulation model.

2.6.2. Influence of cylindrical EWC size on heating uniformity

The effect of cylindrical EWC sizes on RF heating uniformity in potato starch with mid-high moisture was determined. In this study, based on the previously used cross EWC, the heights of cylindrical EWC sheets were swept from 20 mm to 60 mm with an interval of 10 mm for three selected EWC diameters of 76, 96 and 112 mm, which were used both in the experiment and simulation to investigate the effect of cylindrical EWC sizes and make the comparison with the previously used cross EWC on heating uniformity and temperature distribution.

2.7. RF heating time with cylindrical EWC

RF heating rate in samples was largely affected by the EWC size. To make the comparison of the heating effects between the cross EWC and cylindrical EWC, the RF heating time used in this study for each of the experiment was the same with the corresponding cross EWC size. The heating time of each experiment used in this study was listed in Table 2.

2.8. Applications of the cylindrical EWC shape with simulation

To further simplify the EWC structure for practical applications, instead of separating structure of container and EWC, a new hollow cylindrical EWC was designed to form the container and EWC as integral based on computer simulation (Fig. 5). The evaluation and comparison study was conducted in the simulation model between the hollow and solid cylindrical EWC with same sample parameter and geometry EWC size (112 mm diameter with 50 mm height). The material parameters and thickness of hollow cylindrical EWC should be in according with the container (polypropylene) in the simulation model.

2.9. Statistical analysis

The mean values and standard deviation from the simulated results were calculated and analyzed by COMSOL derived values calculator (V4.3a, COMSOL Multiphysics, Burlington, MA, USA) and Excel (Microsoft Office, V2007, Seattle, WA, USA).

3. Results and discussion

3.1. Top electrode voltage estimation

Based on the study of Zhu et al. (2014) and Wang, Zhu, et al. (2015), top electrode voltage can be estimated with anode current of the RF generator by Eq. (8). The anode currents of RF experiments were almost remained at 0.31 A, thus the estimated top electrode voltage was around 5198.3 V. The small variation of anode current was probably caused by the short RF treatment time with little change of the sample moisture content in a closed container.

3.2. Model validation

The top and middle layer surface temperature contours of the RF treated starch sample (31.55% w.b.) with and without EWC sheets obtained from experimental and simulated results were shown in Fig. 6. The features of simulated and experimental contours were in good agreement, based on the comparison of contour lines and average temperatures. The maximum temperature difference in top and middle sample layers was 22.60 °C and 17.80 °C without EWC (Table 3), respectively, and 26.21 °C and 3.52 °C (Table 4) for the sample with cylindrical EWC (diameter 112 mm with height 50 mm). As Fig. 6 shows, the sample with EWC had better heating effect than that without EWC, especially in the middle layer temperature contours. EWC introduced electromagnetic energy and radiated to surrounding samples from inside, which effectively eliminated the cold spot area and improved the surrounding RF heating uniformity.

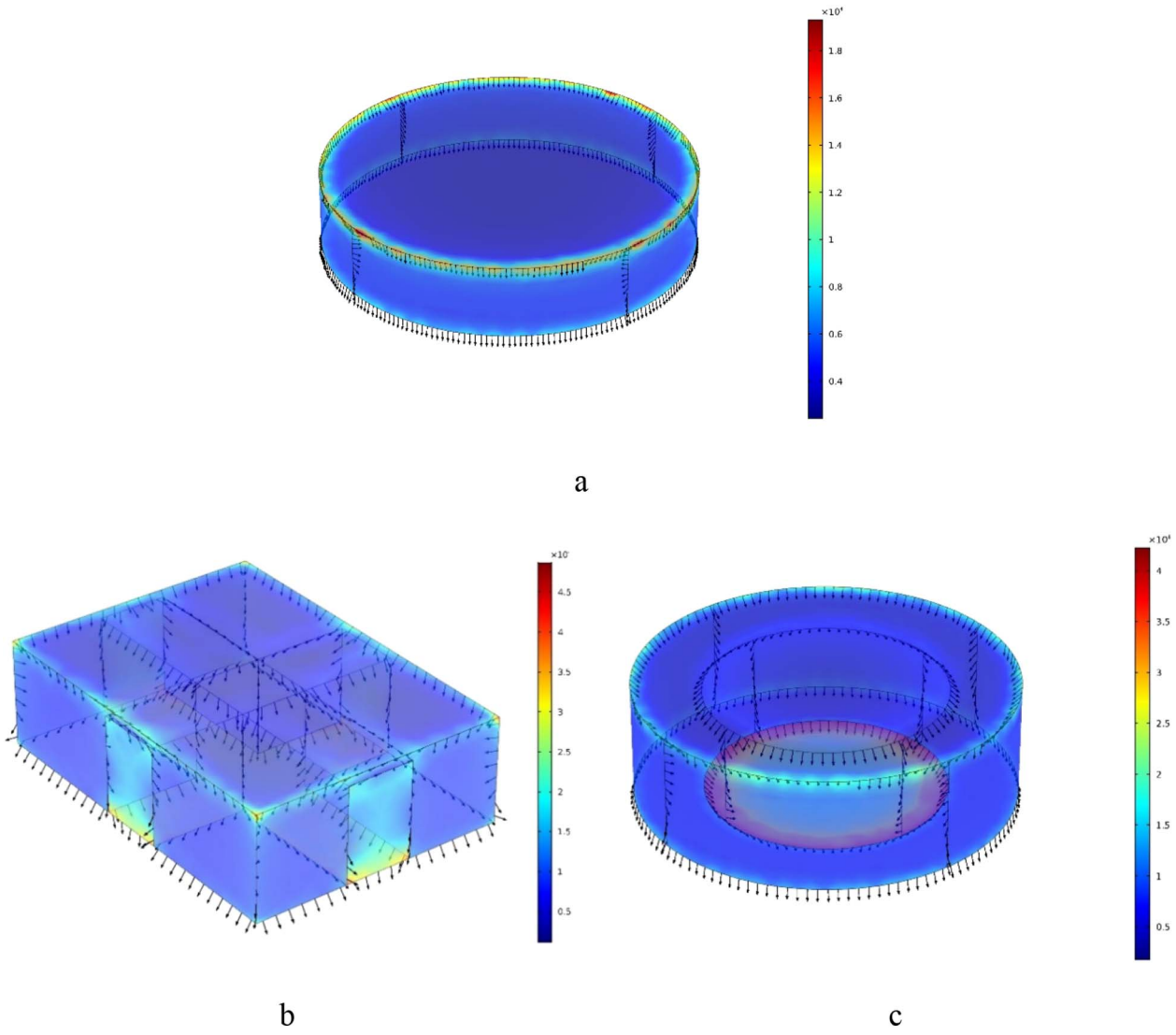

Fig. 7. Electric field intensity (V m^{-1}) and directions in the potato starch sample at terminated time with moisture content of 31.55% treated by RF energy at electrode gap of 110 mm without EWC (a), with cross (b) (35 mm width and 50 mm height) in rectangular containers and cylindrical (c) EWC (112 mm diameter and 50 mm height) in cylindrical containers.

3.3. Effect of EWC on heating patterns and uniformity

3.3.1. Comparison of heating effect of EWC on electric field distribution

Fig. 7 shows the value and direction of electric field intensity in the samples without and with EWC in cross and cylindrical types, respectively. The electric field distribution at cold spot area in the central part of the sample changed obviously and distributed uniformly around the EWC in the sample. The effect of EWC can be described with the function of electromagnetic bending between different materials (TEC, 1987), in which the electromagnetic energy was introduced through the contact area of the sample with EWC and spreading internally to the surrounding part of the sample. As the simulation results indicated, the electric intensity distribution in the cylindrical container with cylindrical EWC (Fig. 7 c) was more uniform than that in the rectangular container with cross EWC (Fig. 7 b) since cylindrical EWC type has less corner and edge parts than cross EWC.

3.3.2. EWC heating effect on overall patterns

Fig. 8 shows the overall temperature distributions of the sample treated without and with EWC sheets in rectangular and cylindrical containers, respectively. For the sample heated without EWC sheets, the cold spot area was largely concentrated at the central area over the whole container (Figs. 8a and c), and the highest temperature parts were focused on the edge of the sample, since the electromagnetic energy always passed through the less resistance parts (Birla et al., 2004). With adding cylindrical EWC (Fig. 8 b) or cross EWC (Fig. 8 d), the overall heating patterns were changed obviously and the temperature distribution in the sample seemed more uniform than that in the sample without EWC, due to the function of the EWC internally modified the electromagnetic distribution. For the sample heated with cross EWC, the volume average temperature of the sample without EWC was 41.57 °C for heating time of 340 s, compared to that of 47.58 °C with EWC in the heating time of 178 s. For the sample heated with cylindrical EWC, the volume average temperature of the sample without EWC

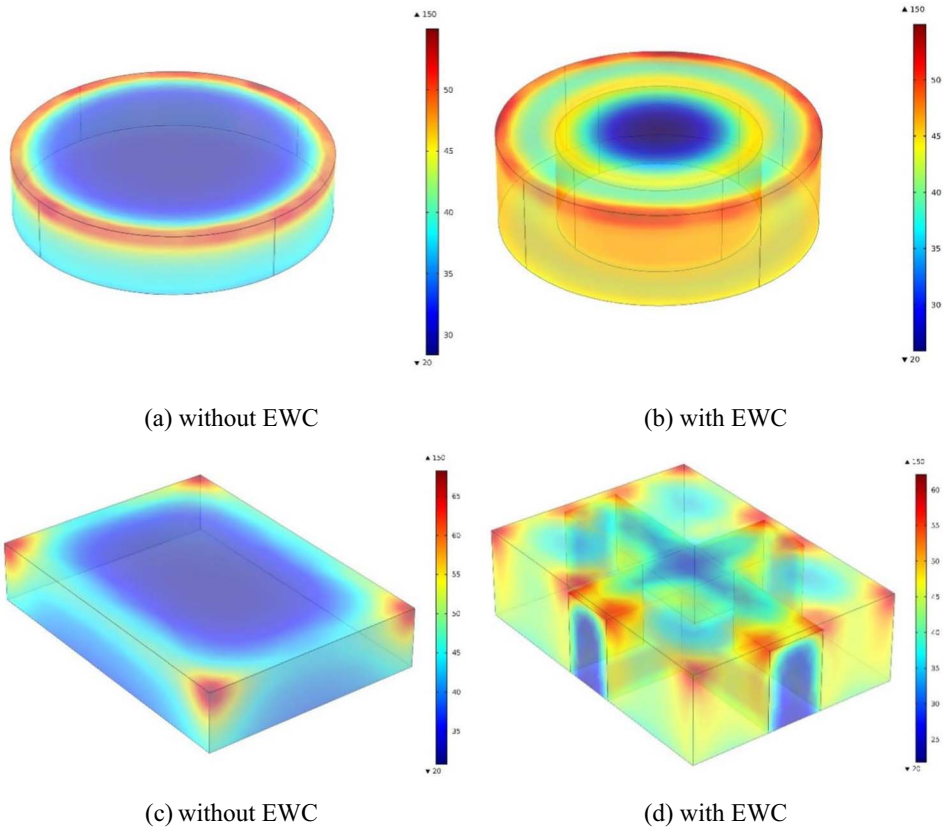

Fig. 8. Overall heating patterns (°C) of the potato starch sample treated by RF energy without (a) and with (b) cylindrical EWC (112 mm diameter and 50 mm height), or without (c) and with (d) cross EWC (35 mm width and 50 mm height) in cylindrical or rectangular containers at electrode gap of 110 mm and initial temperature of 23 °C.

Table 5
Simulated volume average temperature (VAT, °C) and target uniformity index (TUI) of starch with moisture content of 31.55% w.b. with various EWC heights after RF heating with electrode gap of 110 mm.

EWC height (mm)	Parameter	EWC diameter (mm)		
		76	96	112
Without	VAT	36.90		
	TUI	0.595		
20	VAT	40.75	41.24	41.43
	TUI	0.478	0.458	0.458
30	VAT	42.11	42.20	43.97
	TUI	0.438	0.436	0.396
40	VAT	43.37	43.94	44.93
	TUI	0.400	0.383	0.355
50	VAT	43.37	44.59	46.63
	TUI	0.400	0.366	0.313
60	VAT	43.37	44.59	46.05
	TUI	0.400	0.366	0.331

was 36.90 °C with heating time of 340 s, compared to that of 46.63 °C with EWC in the heating time of 178 s. The improvement functions of cylindrical EWC on temperature distribution and heating rate were as obvious as that of the cross EWC, but the volume average temperature of the sample heated with cylindrical EWC (112 mm diameter and 50 mm height) was 0.95 °C lower than that of the corresponding cross EWC (35 mm width and 50 mm height). Table 5 indicated that the TUI decreased from 0.595 to 0.313 as the cylindrical EWC (diameter 112 mm with height 50 mm) was added, resulting in the improved RF heating uniformity.

3.3.3. *Effect of the cylindrical EWC diameter and height*

Figs. 9 and 10 with Tables 3 and 4 show the experimental and simulated temperature contours in top and middle layers of starch with different EWC sizes, which also indicated the agreements between the experiment data and simulation results. As cylindrical EWC diameter increased, increasing electromagnetic energy was introduced into the sample vertically. The average temperature of the middle layer increased from 45.99 to 48.28 °C with the standard deviation decreased from 2.68 to 1.28 °C (Table 3), and TUI decreased from 0.478 to 0.458, from 0.438 to 0.396 and from 0.400 to 0.355, respectively, for the corresponded EWC heights of 20, 30 and 40 mm (Table 5). Figs. 8 and 9 also illustrated the clear improvement of RF heating uniformity. The diameter of cylindrical EWC had positive effects to improve RF heating uniformity. As the cylindrical EWC height increased, increasing electromagnetic energy was introduced into the sample horizontally. The average middle layer temperature increased from 42.87 to 49.24 °C associated with the standard deviation dropped from 7.78 to 0.73 °C (Table 4), and the TUI decreased from 0.478 to 0.400, from 0.458 to 0.366, and from 0.458 to 0.313, respectively, for 3 different EWC diameters of 76, 96 and 112 mm (Table 5). Therefore, the increased EWC height can also improve the RF heating uniformity. In Table 5, when the

height of EWC reached 60 mm for the cylindrical EWC with diameter of 112 mm, the TUI indicated a slight rise from that of the last value, which is same with the previous study (Zhu et al., 2017), but this tendency might be not obvious for the cylindrical EWC with diameters of 76 and 96 mm.

3.4. Heating effects comparison between cylindrical and cross EWC

Tables 6 and 7 indicated the UI values based on Eq. (9) for the potato starch samples treated with cylindrical and cross EWC under same treatment condition. The UI values of sample treated with cylindrical EWC were 0.008, 0.002, 0.005, 0.030 and 0.009 lower than those with cross EWC, respectively, for 5 EWC heights of 20, 30, 40, 50 and 60 mm (Table 6) at determined cylindrical EWC diameter (112 mm) and cross EWC width (35 mm). With determined EWC height of 30 mm, the UI of the sample treated with various cylindrical EWC diameters and cross EWC widths was listed in Table 7. The UI values for cylindrical EWC were 0.051, 0.019 and 0.002 lower than those with cross EWC, respectively, for 3 cylindrical EWC diameters of 76, 96 and 112 mm and the corresponding cross EWC width of 15, 25, and 35 mm. As Tables 3 and 4 showed, the highest temperature in each contour with cylindrical EWC was lower than that of the sample treated with cross EWC. The difference of heating effect between the sample treated with cylindrical EWC and cross EWC can also be directly seen from the temperature contours comparison in Fig. 8 and the temperature deviation comparison in Tables 3 and 4. From infrared imaging data, the top layer temperature difference of the sample treated with cylindrical and cross EWC were 25.44 and 29.49 °C, respectively, for the related

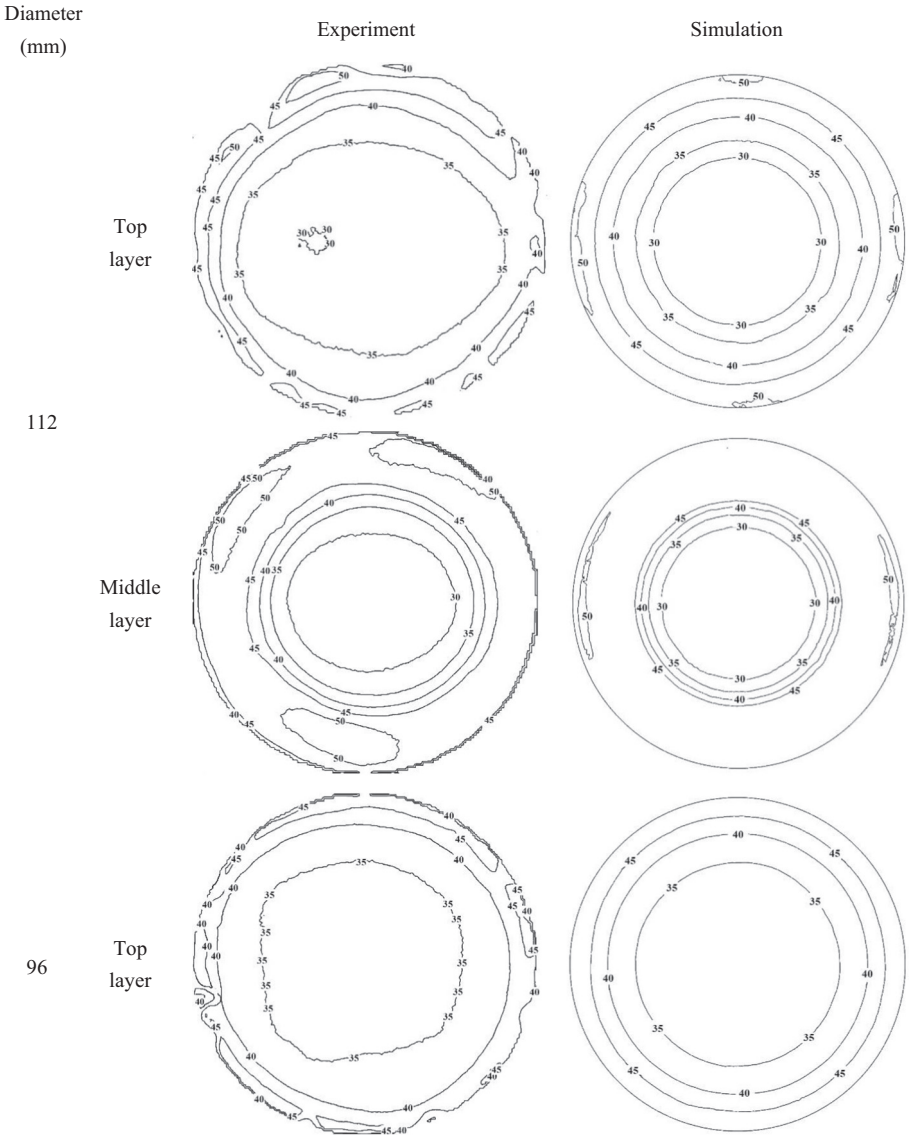

Fig. 9. Simulated and experimental temperature distributions (°C) of potato starch with moisture contents of 31.55% w.b. in top and middle layers placed in the cylindrical polypropylene container on the center of bottom electrode after RF heating at the electrode gap of 110 mm and initial temperature of 23 °C with different EWC diameters (112, 96, and 76 mm) and determined height of 30 mm.

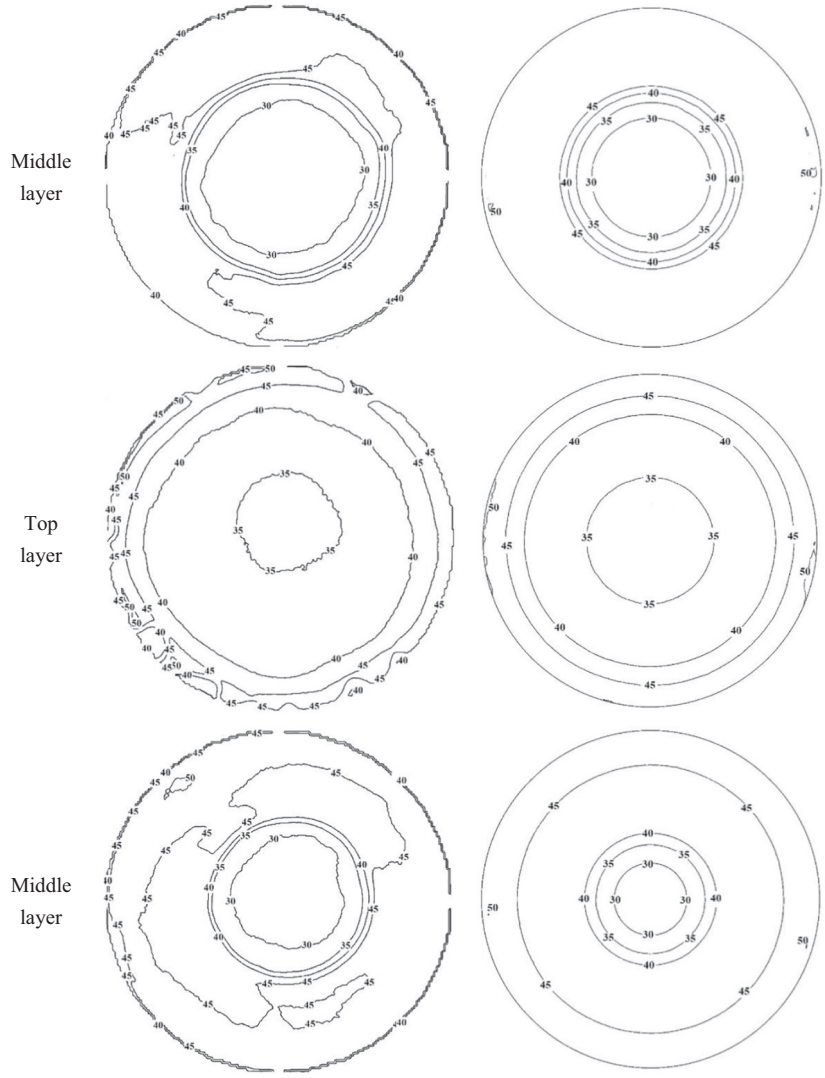

Fig. 9. (*continued*)

cylindrical EWC (diameter 112 with height 50 mm) and cross EWC (width 35 mm with height 50 mm). For the sample treated without EWC, the top layer temperature difference was 17.95 and 27.80 °C for cylindrical container and rectangular container, respectively. Therefore, the sample treated with cylindrical EWC has better RF heating uniformity effect but the lower final temperature than that of the cross EWC, since the cylindrical container and EWC effectively minimized the temperature distributions in corner and edge parts of the sample but reduced the contacting area between the sample and EWC wall.

The decision of these two kinds of EWC is based on the treatment purpose and throughput, the cylindrical one is more suitable for the laboratory scale RF treatment for its feature of stable heating, and the cross one are more suitable for large scale RF treatments, especially for the continuous conveyor treatment with the advantages of fast heating and high throughput.

3.5. Effect of hollow EWC structures

As Fig. 11 shows, the heating patterns in the sample with hollow cylindrical EWC were similar to those with the solid cylindrical EWC. The average temperatures in top and middle layers of the sample with hollow EWC after 178 s RF heating in simulation were 45.16 °C and 50.03 °C with standard deviation of 9.81 °C and 1.94 °C, respectively, compared to 41.59 °C and 49.24 °C with standard deviation of 7.33 °C and 0.73 °C for the sample treated with the solid cylindrical EWC. The volume average temperature and UI value of the hollow EWC were 48.37 °C and 0.138 compared to 46.63 °C and 0.140 for the solid EWC. The average temperature of the sample with hollow cylindrical EWC was higher than that of the solid ones, but the larger layer temperature deviation was found for the sample treated with hollow cylindrical EWC. This may be caused by that the hollow cylindrical EWC gathered

more electromagnetic energy at the interior contacting part of the sample than the solid one, because air has lower dielectric properties and density than Polystyrene (Table 1). Therefore, this new design of the hollow EWC is meaningful for the future EWC type study. Particularly, the hollow EWC type ensured the container wall and EWC combining as an integral, which simplified the manipulation and structure of the EWC.

4. Conclusions

Based on the heating patterns of each experiment, the computer model with new cylindrical EWC heated by RF energy was established and explored to evaluate the heating uniformity improvement with mid-high moisture potato starch samples using COMSOL software. The cylindrical EWC had positive effects on RF heating uniformity by changing the electromagnetic energy distribution inside the sample. The experimental and simulated results showed that the heating uniformity improved as the cylindrical EWC diameter increased, and the best heating uniformity value was obtained at the cylindrical EWC size of 112 mm diameter and 50 mm height based on both TUI and layer temperature comparison. Heating uniformity improving effect of the cylindrical EWC was better than that of the cross EWC based on UI comparison. A new hollow cylindrical EWC was designed and explored by computer simulation to further simplify the EWC structure, and the results indicated that the RF treated sample with hollow cylindrical EWC had a similar overall heating pattern but lower UI than that of the

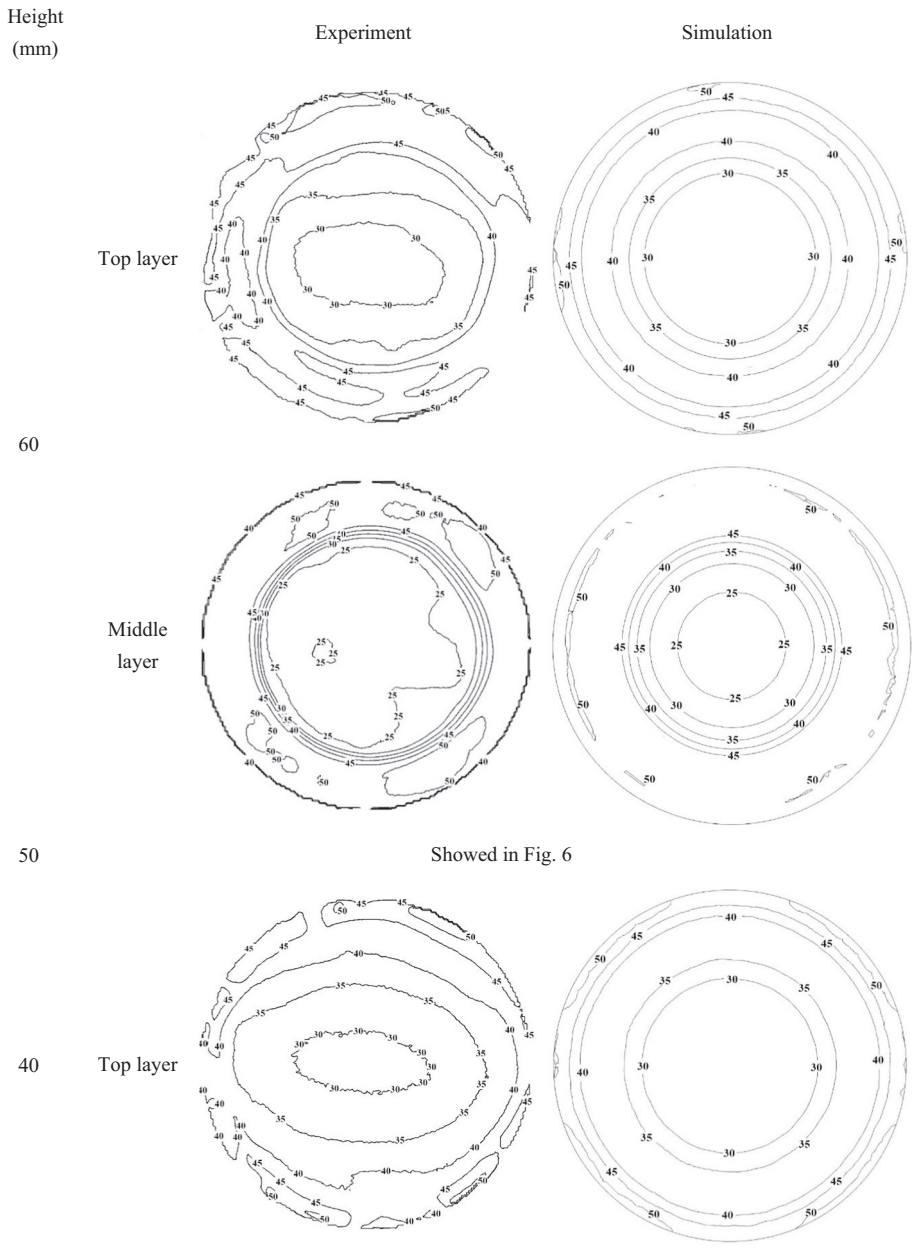

Fig. 10. Simulated and experimental temperature distributions (°C) of potato starch with moisture contents of 31.55% w.b. in top and middle layers placed in the cylindrical polypropylene container on the center of bottom electrode after RF heating at the electrode gap of 110 mm and initial temperature of 23 °C with different EWC heights (20, 30, 40, 50 and 60 mm) at determined diameter of 112 mm.

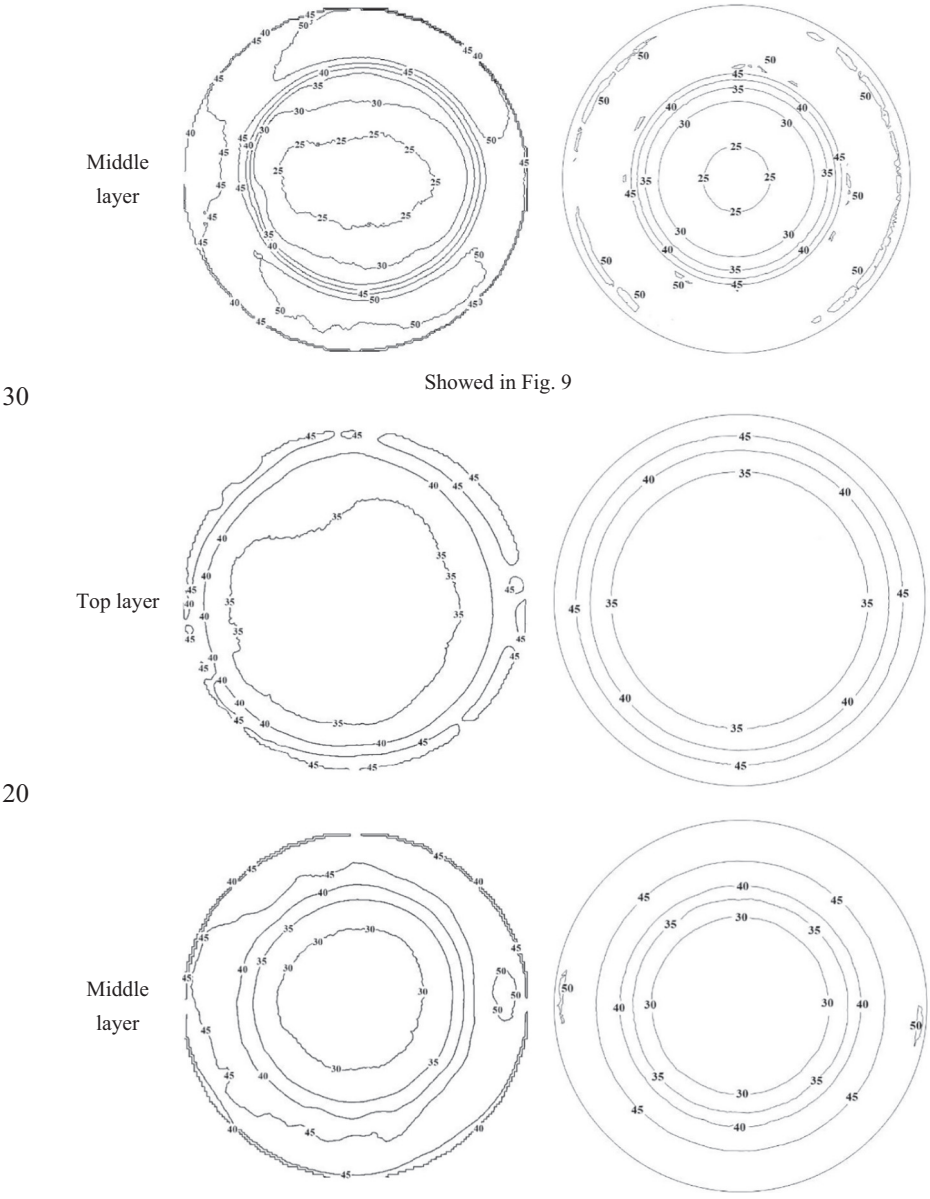

Fig. 10. (*continued*)

Table 6
Simulated uniformity index (UI) of starch at moisture content of 31.55% w.b. with different EWC heights at determined diameter (112 mm) and width (35 mm) for cylindrical EWC and cross EWC, respectively, after RF heating with electrode gap of 110 mm.

EWC height (mm)	UI	
	Cylindrical EWC	Cross EWC
20	0.318	0.326
30	0.298	0.300
40	0.218	0.223
50	0.140	0.170
60	0.128	0.137

Table 7
Simulated uniformity index (UI) of starch at moisture content of 31.55% w.b. with different EWC diameters and widths at determined height (30 mm) for cylindrical EWC and cross EWC, respectively, after RF heating with electrode gap of 110 mm.

Cylindrical EWC diameter (mm)	UI	Cross EWC width (mm)	UI
76	0.170	15	0.221
96	0.250	25	0.269
112	0.298	35	0.300

sample treated with solid cylindrical EWC. This study may provide potential practical applications for improving RF heating uniformity in the treated large-scale mid-high moisture food.

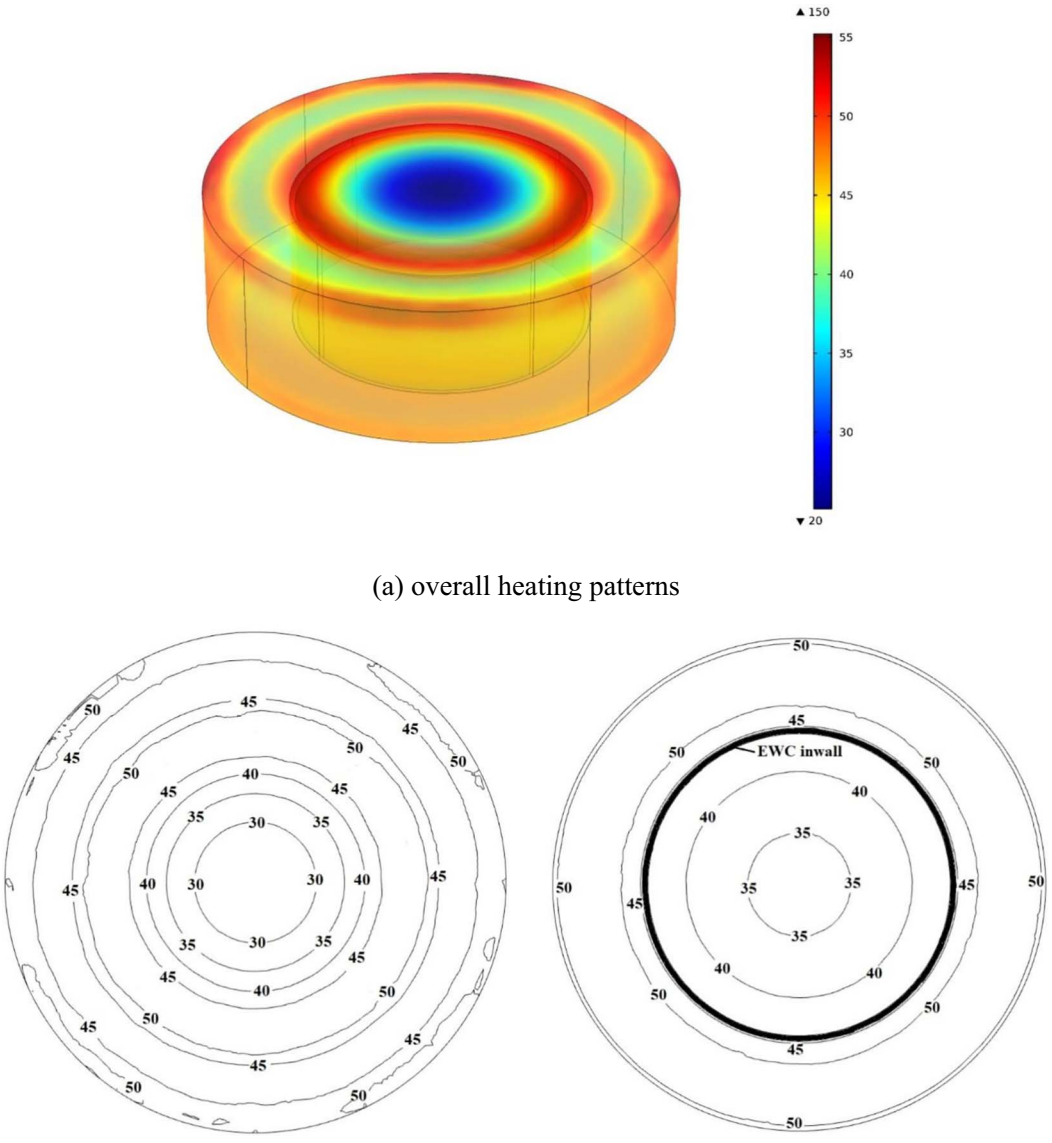

(a) overall heating patterns

(b) top layer

(c) middle layer

Fig. 11. Simulated temperature distributions (°C) of potato starch in volumetric, top and middle layers placed in the specific polypropylene container with hollow EWC on the center of bottom electrode after RF heating at the electrode gap of 110 mm and initial temperature of 23 °C with EWC size of 112 mm diameters and 50 mm height.

Acknowledgements

This research was conducted in the Northwest A&F University and Chinese Academy of Agricultural Mechanization Sciences. This work was supported by the National Key Research and Development Plan (2016YFD0401300; 2017YFD0400900). The authors also thank Rui Li, Bo Zhang, Teng Cheng, Zhi Huang and Bo Ling for their helps in conducting experiments.

References

Alfaifi, B., Tang, J., Jiao, Y., Wang, S., Rasco, B., Jiao, S., & Sablani, S. (2014). Radio frequency disinfestation treatments for dried fruit: Model development and validation. *Journal of Food Engineering, 120*(0), 268–276.

Alfaifi, B., Tang, J., Rasco, B., Wang, S., & Sablani, S. (2016). Computer simulation analyses to improve radio frequency (RF) heating uniformity in dried fruits for insect control. *Innovative Food Science & Emerging Technologies, 37*, 125–137.

Balanis, C. A. (1989). *Advanced engineering electromagnetics.* Canada: John Wiley & Sons.

Bedane, T. F., Chen, L., Marra, F., & Wang, S. (2017). Experimental study of radio frequency (RF) thawing of foods with movement on conveyor belt. *Journal of Food Engineering, 201*, 17–25.

Birla, S. L., Wang, S., Tang, J., & Hallman, G. (2004). Improving heating uniformity of fresh fruit in radio frequency treatments for pest control. *Postharvest Biology and Technology, 33*(2), 205–217.

Brandrup, J., Immergut, E. H., Grulke, E. A., Abe, A., & Bloch, D. R. (1989). *Polymer handbook.* USA: John Wiley & Sons.

Chandrasekaran, S., Ramanathan, S., & Basak, T. (2013). Microwave food processing—A review. *Food Research International, 52*(1), 243–261.

Chen, L., Wang, K., Li, W., & Wang, S. (2015). A strategy to simulate radio frequency heating under mixing conditions. *Computers and Electronics in Agriculture, 118(C,* 100–110.

Choi, C. T. M., & Konrad, A. (1991). Finite element modeling of the RF heating process. *IEEE Transactions on Magnetics, 27*(5), 4227–4230.

COMSOL (2012). *Material library V4.3a. COMSOL multiphysics, Burlington*.

Erdogdu, F., Altin, O., Marra, F., & Bedane, T. F. (2017). A computational study to design process conditions in industrial radio-frequency tempering/thawing process. *Journal of Food Engineering, 213*, 99–112.

Hou, L., Ling, B., & Wang, S. (2014). Development of thermal treatment protocol for disinfesting chestnuts using radio frequency energy. *Postharvest Biology and Technology, 98*, 65–71.

Huang, Z., Zhang, B., Marra, F., & Wang, S. (2016). Computational modelling of the impact of polystyrene containers on radio frequency heating uniformity improvement for dried soybeans. *Innovative Food Science & Emerging Technologies, 33*, 365–380.

Huang, Z., Zhu, H., Yan, R., & Wang, S. (2015). Simulation and prediction of radio frequency heating in dry soybeans. *Biosystems Engineering, 129*, 34–47.

Jiao, Y., Shi, H., Tang, J., Li, F., & Wang, S. (2015). Improvement of radio frequency (RF)

heating uniformity on low moisture foods with polyetherimide (PEI) blocks. *Food Research International, 74*, 106–114.
Jiao, Y., Tang, J., & Wang, S. (2014). A new strategy to improve heating uniformity of low moisture foods in radio frequency treatment for pathogen control. *Journal of Food Engineering, 141*, 128–138.
Juran, R. (1991). *Modern plastics encyclopedia.* USA: McGraw-Hill.
Koral, T. (2004). Radio frequency heating and post-baking. *Biscuit World Issue, 7*(4), 1–7.
Liu, Y., Tang, J., Mao, Z., Mah, J.-H., Jiao, S., & Wang, S. (2011). Quality and mold control of enriched white bread by combined radio frequency and hot air treatment. *Journal of Food Engineering, 104*(4), 492–498.
Marra, F., Zhang, L., & Lyng, J. G. (2009). Radio frequency treatment of foods: Review of recent advances. *Journal of Food Engineering, 91*(4), 497–508.
Nelson, S. O. (1996). Review and assessment of radio-frequency and microwave energy for stored-grain insect control. *Transactions of ASAE, 39*(4), 1475–1484.
TEC (1987). *Radio frequency dielectric heating in industry.* Palo Alto, USA: Thermo Energy Corporation [pp. c1-c6].
Tiwari, G., Wang, S., Tang, J., & Birla, S. (2011a). Analysis of radio frequency (RF) power distribution in dry food materials. *Journal of Food Engineering, 104*(4), 548–556.
Tiwari, G., Wang, S., Tang, J., & Birla, S. L. (2011b). Computer simulation model development and validation for radio frequency (RF) heating of dry food materials. *Journal of Food Engineering, 105*(1), 48–55.
Uyar, R., Erdogdu, F., Sarghini, F., & Marra, F. (2016). Computer simulation of radio-frequency heating applied to block-shaped foods: Analysis on the role of geometrical parameters. *Food and Bioproducts Processing, 98*(Supplement C), 310–319.
Von Hippel, A. (1954). *Dielectric properties and waves.* USA: John Wiley & Sons.
Wang, K., Chen, L., Li, W., & Wang, S. (2015). Evaluating the top electrode voltage distribution uniformity in radio frequency systems. *Journal of Electromagnetic Waves and Applications, 29*(6), 1–11.
Wang, K., Zhu, H., Chen, L., Li, W., & Wang, S. (2015). Validation of top electrode voltage in free-running oscillator radio frequency systems with different moisture content soybeans. *Biosystems Engineering, 131*, 41–48.
Wang, S., & Tang, J. (2001). Radio frequency and microwave alternative treatments for insect control in nuts: A review. *Agricultural Engineering Journal, 10*(3&4), 105–120.
Wang, S., Tiwari, G., Jiao, S., Johnson, J. A., & Tang, J. (2010). Developing postharvest disinfestation treatments for legumes using radio frequency energy. *Biosystems Engineering, 105*(3), 341–349.
Wang, Y., Li, Y., Wang, S., Zhang, L., Gao, M., & Tang, J. (2011). Review of dielectric drying of foods and agricultural products. *International Journal of Agricultural and Biological Engineering, 4*(1), 1–19.
Zhang, B., Zheng, A., Zhou, L. Y., Huang, Z., & Wang, S. J. (2016). Developing hot air-assisted radio frequency drying protocols for in-shell walnuts. *Emirates Journal of Food & Agriculture, 28*(7), 459–467.
Zhang, S., Huang, Z., & Wang, S. (2017). Improvement of radio frequency (RF) heating uniformity for peanuts with a new strategy using computational modeling. *Innovative Food Science & Emerging Technologies, 41C*, 79–89.
Zheng, A., Zhang, L., & Wang, S. (2017). Verification of radio frequency pasteurization treatment for controlling *Aspergillus parasiticus* on corn grains. *International Journal of Food Microbiology, 249*, 27–34.
Zhu, H., Huang, Z., & Wang, S. (2014). Experimental and simulated top electrode voltage in free-running oscillator radio frequency systems. *Journal of Electromagnetic Waves and Applications, 28*(5), 606–617.
Zhu, H., Li, D., Li, S., & Wang, S. (2017). A novel method to improve heating uniformity in mid-high moisture potato starch with radio frequency assisted treatment. *Journal of Food Engineering, 206*, 23–36.